



HAL
open science

PREDICTION OF ARREST PRESSURE IN PIPE BASED ON CTOA

M Ben Amara, G Pluvinage, Julien Capelle, Z Azari1

► **To cite this version:**

M Ben Amara, G Pluvinage, Julien Capelle, Z Azari1. PREDICTION OF ARREST PRESSURE IN PIPE BASED ON CTOA. Journal of Pipeline Integrity, 2015. hal-02972903

HAL Id: hal-02972903

<https://hal.science/hal-02972903>

Submitted on 20 Oct 2020

HAL is a multi-disciplinary open access archive for the deposit and dissemination of scientific research documents, whether they are published or not. The documents may come from teaching and research institutions in France or abroad, or from public or private research centers.

L'archive ouverte pluridisciplinaire **HAL**, est destinée au dépôt et à la diffusion de documents scientifiques de niveau recherche, publiés ou non, émanant des établissements d'enseignement et de recherche français ou étrangers, des laboratoires publics ou privés.

PREDICTION OF ARREST PRESSURE IN PIPE BASED ON CTOA

M.Ben amara¹, G.Pluinage², J.Capelle¹, Z.Azari¹

¹LaBPS – ENIM, 1 route d’Ars Laquenexy, CS 65820, 57078 Metz, France

²FM.C 57530 Silly Sur-Nied, France

Corresponding author: mohamed.ben.amara.enim@gmail.com

Abstract

Crack extension modelled by Finite Element method using CTOA criterion coupled with the the node release technique is used to predict the crack velocity, the arrest pressure and crack length. This method is compared with the different Two Curves Methods Batelle, HLP and HLP-Sumitomo and is close to the last one for two pipe steels API5L X65 and X100. Influence of pipe thickness is studied through the concept of triaxial stress constraint. This method confirms also that the arrest pressure decreases exponentially with the square root of the diameter.

1. INTRODUCTION

Gas pipeline fracture initiation is usually followed by extended running crack propagation. Such disasters lead to significant financial loss, and should be avoided as much as possible or confined to a short portion of the pipe. Therefore, an important question is whether and when the fracture will self-arrest.

Even if brittle crack propagation can be successfully avoided by using high toughness steel, the running ductile fracture remains the most important failure mode in modern gas pipelines [1]. It occurs when driving force energy, caused by internal pipe pressure, overcomes the crack propagation toughness.

In fracture mechanics, the crack resistance growth can be expressed by the experimental crack growth resistance curve (R-Curve), crack tip opening displacement (CTOD) or crack tip opening angle (CTOA) interconnected parameters based on the crack extension Δa . In terms of a limit state design, the arrest pressure can be predicted by solving the equality (1) between the fracture toughness and component stress which depend on the pipeline dimensions, internal pressure and material strength. This material resistance is balanced with a component stressing which is determined involving specific pipe dimensions, pressure p and material strength. In terms of a limit state design, the arrest pressure can be predicted by solving the equality between the stress state at crack tip :

$$\langle \sigma_{ij}(p) \rangle = \langle \sigma_{ij,c}(p_{ar}) \rangle \quad (1)$$

where p_{ar} is the pressure at arrest. Condition of arrest can be transformed by the new following condition :

$$CTOA(p) = CTOA_c(p_{ar}) \quad (2)$$

where CTOA is the crack tip opening angle induced by the current pressure and $CTOA_c$ the fracture toughness.

Conditions for crack propagation or arrest are given by a coupled fluid-structure problem. Depressurization due to crack opening will cause fluid flow out of the pipe. This induces a depressurization waves propagating in opposite directions from the tips of the opening crack.

Crack propagation speed is controlled by pressure distribution on the opening pipe. If the decompression wave is faster than the propagating crack fracture, the pressure at crack tip will decrease and crack arrest.

In the standard codes for gas transmission pipelines, the toughness requirement for crack arrest is based on models which express the fracture resistance and driving force in terms of the fracture and gas decompression wave velocities. This approach involves the superposition of two curves: the gas decompression wave speed and the ductile fracture propagation speed characteristic, each as a function of the local gas pressure. For this reason, they are called Two Curves Method (TCM).

In the present work, the crack arrest criterion, given by equation (2), is extended to the two-curve method through an FE simulation model in conjunction with the node release technique. This method is used for the prediction of crack velocity, pressure at arrest and crack length after arrest by numerical simulation of two pipe steels API X and X100. A comparison is made with the HLP-Sumitomo model two curves models for crack arrest [2].

2. CRACK-TIP OPENING ANGLE (CTOA) OF API 5L X65 AND X100 STEELS

CTOA is conventionally defined as the angle comprise between two lines emanating from crack tip and intercepting the crack profile at a conventionally distance Δa^* with $0.5 < \Delta a^* < 1.5$ mm. The crack length Δa^* depends on the condition of the crack surface. Several experimental methods have been proposed for measuring CTOA, for example, optical microscopy [3], image correlation [4], microtopography [5], the δ_5 technique [4] and interpolation from the force-displacement curve [6].

Experimental determination of CTOA on API 5L X65 has been performed on A modified Compact tension (CT) specimen . Design and geometry dimensions of the test specimen is shown in Figure 1. The specimens was pre-cracked to provide an initial crack length to specimen width ratio of $a/W=0.4$.

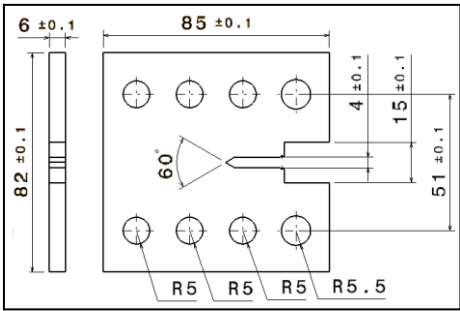


Fig.1 Geometry of modified CT specimen used for CTOA determination

A commercial Digital Image correlation (DIC) camera and an software analysis package with integrated length and angle measurement tools is used to measure CTOA and crack extension Δa . The recording time is automatically available from the videotapes where a digital stopwatch was used to synchronize the still images. All of this allowed the correlation between test parameters such as load, displacement, crack length Δa and CTOA. The recorded video was transformed into an image sequence file then 25 of this images are selected to

measure the evolution of CTOA as a function of crack extension Δa . According to ASTM (E 2472) [7] requirements the CTOA measurements were made at a distance behind the crack tip ranging between 0.5 and 1.5 mm.

A second method involve to reproduce experimental test by combining experimental load-deflection data and finite element analysis then measure the evolution of a CTOA numerically (Combining Numerical Method CN).

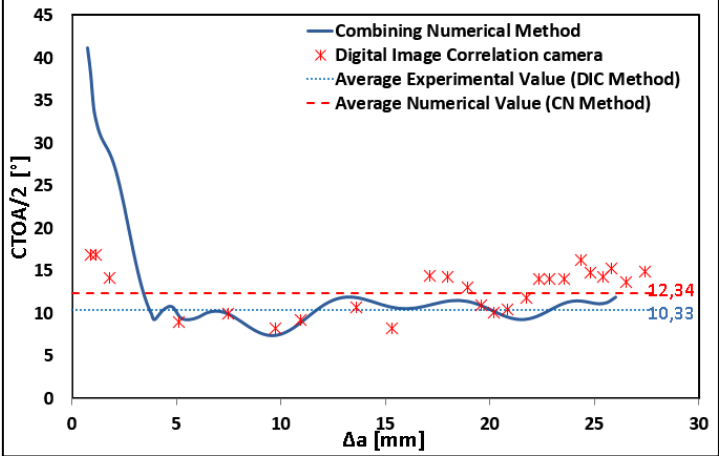


Fig.2 the CTOA vs. crack extension for API5L X 65 pipe steel measured on a modified CT specimen with 6mm thickness.

In Fig.2, the CTOA vs. crack extension data obtained from modified CT specimens using the DIC method and CN method. As we observe, the DIC measured data do not exhibit the initial rapid decrease in CTOA, however they are quite comparable to the CTOA measurements obtained using the CN method in the constant CTOA range. Consequently, the second method offers more advantage in its accuracy, as well as in its implementation. For all experimental tests, the CTOA vs. crack extension behaviour consisted of an initially high CTOA region that quickly transitioned into a clearly constant CTOA region corresponding to a steady state for crack growth. According to S. Lam [9] , it is recommended to take account of the initial values of CTOA for predicting crack growth. Consequently, a bilinear form of CTOA has been defined by fitting the CTOA experimental curve results then introduced in the Numerical simulation

The CTOA experimental results are reported in Fig .2, and an average constant $CTOA_c$ is set as 20° . This value is compared with other values of $CTOA_c$ found in literature (table 4).

Table 4 values of $CTOA_c$ found in Literature and in the present study for API 51 X65 and X100 steel.

References	Material	Yield stress (MPa)	$CTOA_c$ (°)	Thickness (mm)
O'Donoghue et al [9]	X65	447	8,1	18
O'Donoghue et al [9]	X65	529	14,2	18
Present study	X65	465	20	6
[10]	X100	734	14	na

One notes the high value of the CTOA of API X65 measured in the present study and the low thickness (6 mm) of the specimen. Constraint effect explains probably this high value.

3. MODELLING CRACK EXTENSION IN A PIPE UNDER INTERNAL PRESSURE

3.1 Modelling of crack extension

Crack extension is modelled by the finite element method using the CTOA criterion coupled with the node release technique. The node release technique algorithm has been presented in a nearlier study [11]. It is based on the assumption that cracks grow step by step, and each step has the length of one mesh element.

Boundary conditions were imposed on the pipe in order to make the simulation as real as possible. They consisted of imposing symmetry along the crack plane and constraining the closed part of the crack with fixed nodes in the circumferential direction. These fixed nodes were then removed by the nodal release user subroutine to provoke crack extension.

Acting tractions on uncoupling nodes at the crack faces are reduced as the crack opens. This event occurs when CTOA reaches its critical value, and then the representative node of the crack tip is released and the new position of the crack is deduced. This algorithm requires several time increments and a fine mesh (element size under 1.5 mm) around the crack tip for accurate evaluation of the CTOA.

In this approach, the evolution of the crack strictly depends on the mesh element size around the crack tip, since it governs the amount of the crack advance. Moreover, the advancing process is not really continuous since a proper iteration scheme is necessary to evaluate the dynamic crack growth accurately during the integration time.

4.2 Numerical simulation of crack arrest

Crack arrest in gas pipelines was performed with the release user subroutine, in conjunction with the FEM Abaqus code. The computing phase begins by generating a 3D finite element implicit dynamic analysis. Because of the symmetry of the crack planes, only a quarter of the pipeline was analysed. A combined 3D-shell mesh was used to reduce the computing time. A total of 50976 eight node, hexahedral elements were generated along the crack path and combined with 6000 shell elements, as shown in Fig.3.

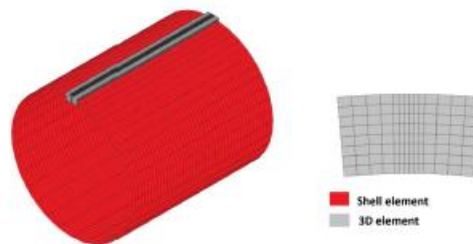


Fig.3 :Combined Shell-3D mesh for numerical simulation of running crack extension

Instantaneous internal pipe pressure was imposed along a certain distance behind the crack-tip node. This distance was given by the cohesive zone model of Dugdale-Barenblatt [12]. The distance is $2b = 3\sqrt{R \cdot t}$ where R and t are outer radius and wall thickness, respectively.

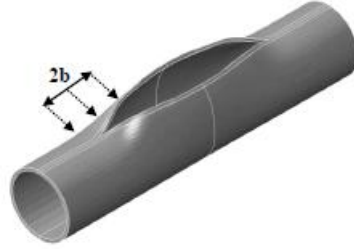


Fig.4 .Zone length where gas pressure is imposed on coupled nodes.

Intensity of this pressure is given by the decompression wave. A simplified gas depressurization model is adopted in this work and assumes that the gas decompression depends only on time and distance from the crack tip. These assumptions are justified by the fact that crack propagation cannot outrun the decompression wave. This means that the crack tip is always present in pipe section affected by the decompression process. Secondly, the expansion of ideal gas is isentropic, the pipe is considered as a large pressure vessel with constant volume. The drop pressure ahead the running crack tip is given by equation as:

$$p(t) = p_0 \cdot \exp(kt) \quad (3)$$

where k is a constant $k=-7.5$ [13] that can be related to the gas parameters and initial conditions of pressure and temperature. The simulation is performed on a pipe of 393 mm outer diameter, 19 mm wall thickness and 6 m length. The pipe was made of API 5L X65 steel with a critical CTOA value of 20° or API 5L X100 steel with a critical CTOA value of 14°

3.3 Mesh dependence

In order to ensure the relevance of the proposed modelling results, it is essential to quantify the mesh dependence. Therefore three different 3D meshes were created. Results presented in Table 5 indicate that a good convergence can be obtained by observing a minimum level of mesh refinement. This level may be related to the definition of the CTOA and the maximum size element cannot exceed 1.5mm.

Table 5. Influence of mesh refinement on crack velocity obtained by node release technique.

	Number of nodes	Number of elements	Element Size (mm)	Working time (h)	Crack velocity [m/s]
Mesh 1	48196	36181	3	32	266.85
Mesh 2	75748	57277	1.4	50	264.13
Mesh 3	237717	189085	0.7	210	260.89

3.4 Strain rate dependence

During running ductile a high strain rate ahead of the crack tip in a pipe submitted to internal pressure has been pointed out numerically. Therefore, a strain rate dependant constitutive equation is used. The Johnson Cook plastic law relationship (eq.4) was introduced therefore in the Abaqus simulation model.

$$\sigma_{eq} = (A + B \varepsilon_{eq})(1 + C \ln \frac{\dot{\varepsilon}_{eq}}{\dot{\varepsilon}_0}) \quad (4)$$

where σ_{eq} is the equivalent stress, ε_{eq} is the equivalent plastic strain, $\dot{\varepsilon}_{eq}$ is the equivalent plastic strain rate and $\dot{\varepsilon}_0$ is the reference strain rate. A, B, C and n are material The Johnson Cook parameters are reported from an earlier study in the literature [14].

Table 6 Johnson Cook parameters for API 51 X65 pipe steel

Material parameters	A (MPa)	B (MPa)	n	C	$\dot{\epsilon}_0$ (s ⁻¹)
	465.5	410.83	0.4793	0.0104	0.000806

The simulation results obtained with and without strain rate dependence indicate that the effect of the strain rate on crack extension is less than 10%,

4. RESULTS

Crack extension modelled by Finite Element method using CTOA criterion coupled with the the node release technique allows to predict the crack velocity, the arrest pressure and crack length. It has been applied for a pipe with wall thickness equal to $t = 19$ mm and external diameter $OD = 355$ mm made in API L X65.

4.1 Crack velocity

Crack extension from an initial crack like defect is computed using the described model. Running crack propagation along the tube consists of two stages, a boost phase where the crack reaches its full velocity in few milliseconds, followed by a steady stage at constant speed. The absence of a deceleration phase is explained by the absence of a pressure drop .

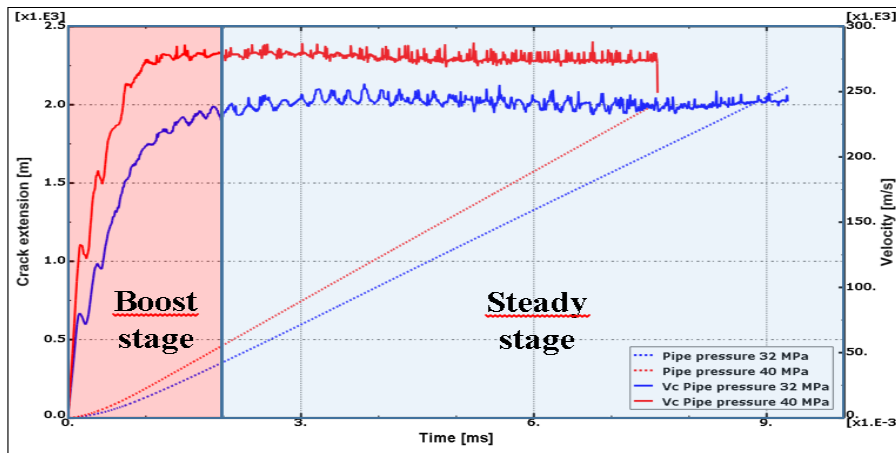


Fig 5: crack extension versus time simulation using CTOA Abaqus User Subroutine.

Fig.5 shows typical simulation results for two initial pressures $p_0= 32$ MPa and $p_0=40$ MPa. One notes that the crack velocity increases with the initial pressure. Ten simulations were performed at different levels of pressures in the range [25 - 60 MPa]. Results indicate that the stationary crack velocity V_c [m/s] increases with initial pressure p_0 in MPa according to :

$$V_c = 290 * \left(\frac{p_0}{24} - 1\right)^{0.14} \quad (5)$$

4.2 Arrest pressure

The arrest pressure is obtained by using the CTOA Abaqus user subroutine within a static analysis.

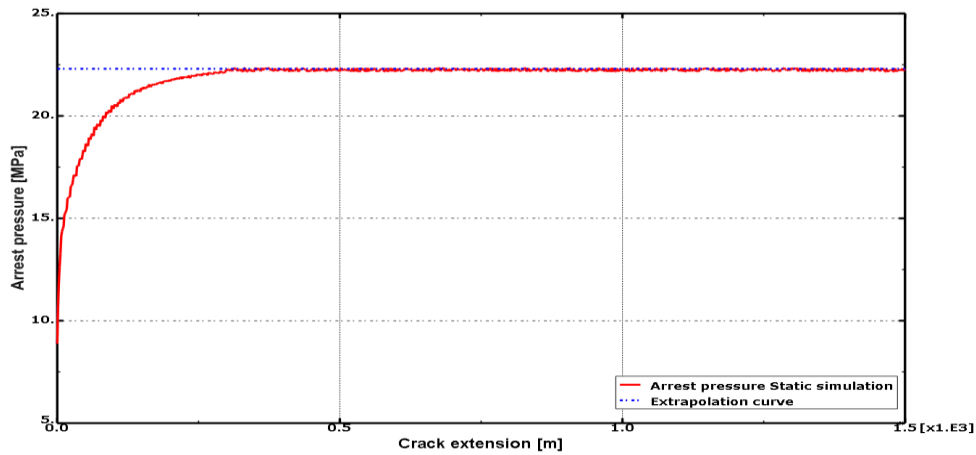


Fig.12 : determination of arrest pressure by static analysis using CTOA Abaqus User Subroutine.

Here the arrest pressure is defined relatively to crack propagation and not arrest. Therefore it is considered as the minimum pressure level to ensure the steady crack propagation. Above this pressure p_{ar} , the crack propagates in instable manner and along a long distance. Under this value, the crack propagation will auto-arrest or propagates along a short distance.

A numerical simulation at initial pressure equal to $p_0 = 22$ MPa, lower than the arrest pressure has been performed and presented in fig 6. In this figure, one notes the absence of steady crack propagation and a quick crack arrest after 9ms. The crack extension is less than 0.5 m.

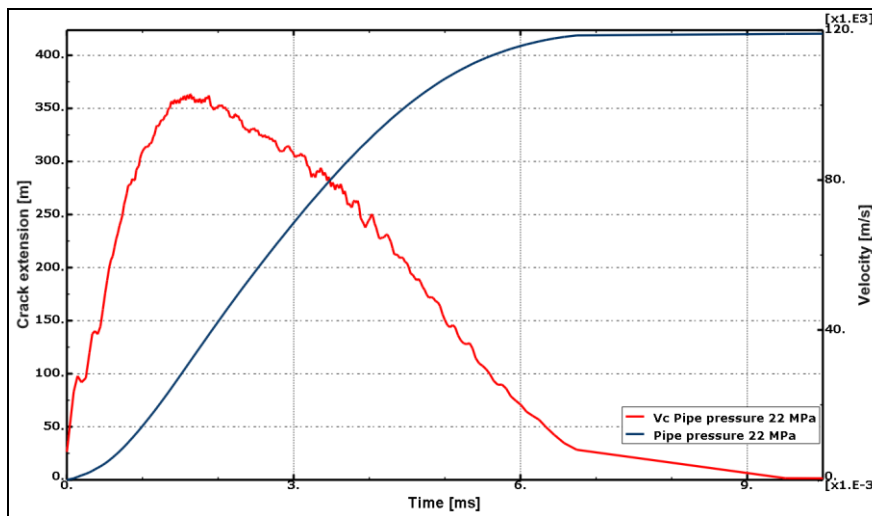


Fig. 6 : rapid crack arrest under initial pressure less than arrest pressure, simulation by numerical analysis using CTOA Abaqus User Subroutine.

4.3 crack extension at arrest

Crack extension at arrest is obtained from the graph crack velocity half of the crack extension to take into account the symmetry of the problem. For the above mentioned conditions of geometry, material and initial pressure, the numerical simulation gives a crack extension of 42 meters which is of the same order of magnitude than those obtained experimentally

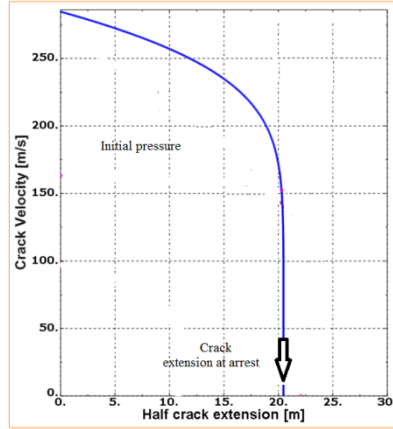


Fig. 7: graph crack velocity half of the crack extension , determination of crack extension at arrest X65 pipe steel, initial pressure $p_0=45$ MPa .

5. DISCUSSION

5.1 Comparison with BTCM, HLP and modified HLP Two Curves Methods

It was proof, by Battelle [1], that the ratio between gas decompression wave and crack propagation speed has major role in the dynamics of crack growth. Indeed, if the crack propagates faster than decompression wave, the crack tip is always loaded by the initial pressure p_0 . Otherwise the crack tip is progressively less and less loaded up to crack arrest.

Gas decompression curve : During the crack propagation process, the gas escapes through the opening created in the wall of the pipe by the crack. Indeed, a decompression wave begins to propagate through the pipe at a speed of the order 300 to 400 m/s. A number of models have been developed for predicting the gas decompression wave speed. Many of the models assume a one-dimensional (along the pipe axis) and isentropic flow and use the Finite Difference Method (FDM) or the Method of Characteristics (MOC). BTCM is a model which assumed one-dimensional, frictionless, isentropic and homogeneous fluid and uses the Benedict -Webb-Rubin-Starling (BWRs) Equation of State (EOS) with modified constants to estimate the thermodynamic parameters during the isentropic decompression

According to this one-dimensional flow model analysis and experimental results obtained from shock tube tests, the decompression pressure at crack tip p_d is given by relationship:

$$\frac{p_d}{p_0} = \left(\frac{V_d}{6V_a} + \frac{5}{6} \right)^7 \quad (6)$$

where p_0 is the initial pressure, V_d decompression gas speed, and V_a acoustic speed.

Crack velocity curve :The crack velocity curve $V_c = f(p_d)$ is given by equ.7 after the analysis of full scale test by Batelle for buried pipelines. It depends on fracture resistance through C_v the Charpy Vee notch upper-shelf energy for a 2/3-thickness specimen and expressed in Joules.

$$V_c = 2.76 \cdot \frac{\sigma_0}{\sqrt{C_v}} \cdot \left(\frac{p_d}{p_a} - 1 \right)^{1/6} \quad (7)$$

where σ_0 is the flow stress. The minimum C_v upper-shelf energy was used in the calibration of the model for arrest. That work was conducted in the late 1960's involving X52 to X65 grade pipes with relatively low Charpy upper-shelf energies.

The Battelle-TCM is still used frequently today. Nevertheless, as higher-grade steels have been developed, it is found from full- scale tests that a multiplier was needed on the minimum Charpy arrest energy calculated from the Battelle-TCM. Several researchers have also suggested that a correction factor was needed on the Charpy energy as the Charpy energy value increased above a certain level. The arrest pressure is given by :

$$p_a = \frac{4}{3.33\pi} \cdot \frac{t}{D} \cdot \sigma_0 \cdot \cos^{-1} \exp\left(\frac{-18.75 \cdot \pi E \cdot C_v}{24\sqrt{Dt/2\sigma_0^2}}\right) \quad (8)$$

where D is the outer diameter of the pipe (mm) and t the pipe wall thickness (mm).

In HLP method [16] , pre-crack Drop Weight Tear Test (DWTT) absorbed energy has been proposed as a better indicator to express resistance to fracture propagation, as the similar fracture surface of running ductile fracture. The wall thickness of DWTT specimen is chosen equal to the pipe thickness. The crack velocity curve $V_c = f(p_d)$ is given by equ.9.

$$V_c = 0.670 \cdot \frac{\sigma_0}{\sqrt{R_f}} \cdot \left(\frac{p_d}{p_a} - 1\right)^{0.393} \quad (9)$$

Fracture resistance R_f is taken as the ratio of D_{DWTT} energy and the pre-cracked test specimen area A_{DWTT} .

The issue of HLP-Sumitomo Method [2] is to correct the arrest energy of high strength line pipe, which is underestimated by HLP method in high pressure pipes. The new equation was developed based on X70 grade pipe of 48 inch OD and extend on higher grade up to X100, the test data of past full scale test on high strength line pipe was taken into consideration. The new crack velocity curve is given as equation (6):

$$V_c = \alpha \cdot \frac{\sigma_0}{\sqrt{R_f}} \cdot \left(\frac{p_d}{p_a} - 1\right)^\beta \quad (10)$$

$$\alpha = 0.670 * [(Dt)/D_0 t_0]^{1/4} \beta = 0.393 * (D/D_0)^{5/2} * (t/t_0)^{-1/2}$$

D_0 and t_0 are reference dimensions $D_0 = 1219.2 \text{ mm}$ and $t_0 = 18.3 \text{ (mm)}$. The crack arrest pressure is given by equ. (7)

$$p_a = \gamma \cdot 0.380 \cdot \frac{t}{D} \cdot \sigma_0 \cdot \cos^{-1} \exp\left(\frac{-4.57 * 10^7 \cdot C_v}{\sqrt{Dt/2\sigma_0^2}}\right) \quad (11)$$

with γ

$$\gamma = 3.42 * \left[3.22 + 0.20 \left(\frac{t/D}{t_0/D_0} \right)^3 \right]^{-1} \quad (12)$$

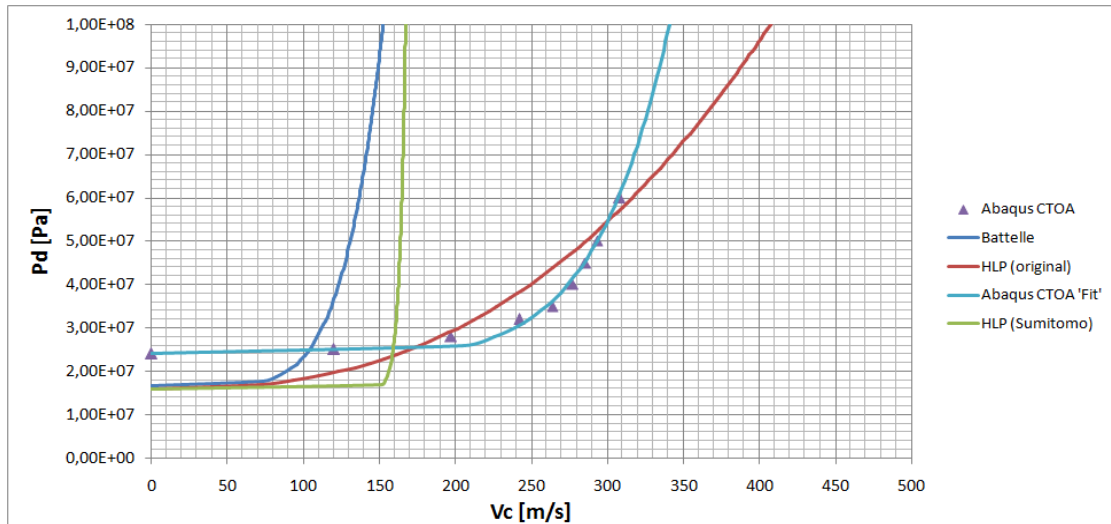


Fig.8 Comparison of CTOA, BTCM, HLP and modified HLP Two Curves Methods
Pipe Outer diameter D393 mm made in API 5L X65 pipe steel.

In the following section, the TCM HLP, HLP-Sumitomo and CTOA Two Curves Method are compared using the following data $D_{DWT} = 280$ J for HLP and HLP-Sumitomo and CTOA = 20° . The resulting crack velocity curves are reported in Table 9 and Fig.8. Therefore predictions of arrest pressure and crack extension are obtain and reported in Table 10
Table 9 : Analytic and numerical equations of crack velocity curves from BTCM, HLP , HLP-Sumitomo and CTOA models.

Model	Analytic equation	Numerical Equation for X65
BTCM	$V_c = 0.379 \cdot \frac{\sigma_0}{\sqrt{R_f}} \cdot \left(\frac{p_d}{p_a} - 1\right)^{1/6}$	$V_c = 90.2 * \left(\frac{p_0}{16.6 * 10^6} - 1\right)^{1/6}$
HLP	$V_c = 0.670 \cdot \frac{\sigma_0}{\sqrt{R_f}} \cdot \left(\frac{p_d}{p_a} - 1\right)^{0.393}$	$V_c = 211 * \left(\frac{p_0}{15.84 * 10^6} - 1\right)^{0.39}$
HLP-Sumitomo	$V_c = \alpha \cdot \frac{\sigma_0}{\sqrt{R_f}} \cdot \left(\frac{p_d}{p_a} - 1\right)^\beta$	$V_c = 161 * \left(\frac{p_0}{15.86 * 10^6} - 1\right)^{0.023}$
CTOA		$V_c = 290 * \left(\frac{p_0}{24 * 10^6} - 1\right)^{0.14}$

Table 10 : predictions of arrest pressure and crack extension from BTCM, HLP , HLP-Sumitomo and CTOA models for API5L X65 pipe steel.

Model	Arrest Pressure (MP0)	Crack extension at arrest (m)
BTCM	16.6	23.8
HLP	15.84	40.7
HLP-Sumitomo	15.86	39
CTOA	23	32.1

These results prove that:

- Results obtained in this study are in agreement with the results of HLP-Sumitomo model.
- The BTCM model underestimates arrest pressure and crack extension at arrest. This inconvenient is not taken into consideration in the present CTOA approach which represents probably a future way to predict crack-arrest in pipe lines.
- HLP's equation overestimated the crack propagation velocity and its extension, this could be explained by the fact that HLP Model has not been validated for smaller pipe diameter. HLP parametric correction is therefore insufficient.
- One has to notes that HLP-Sumitomo model use not a material intrinsic curve of crack velocity but a curve which depends strongly of pipe geometry (outer diameter and thickness). HLP was extended with more parameters in the Sumitomo version. This correction is doubtful since it is only based on pipe geometrical reference point (outer diameter and thickness) instead of the material mechanical intrinsic properties, which implies a deviation in smaller pipelines
- The presented CTOA approach results show a significant gap, over 35%, in the prediction of the arrest pressure compared with those obtained by HLP methods. This drawback is not taken into consideration in the present CTOA approach which probably represents the best way to predict crack-arrest in pipelines.

5.2 Influence of material

Using Crack extension modelled by Finite Element method using CTOA criterion coupled with the the node release technique, decompression pressure versus crack velocity for API 5L X65 and X100 pipe steels have been computed. Stress strain curve of these steel a ben reported in Fig.9 Yield stress, critical CTOA and D_{DWT} energy of these two steels are reported in Table 11.

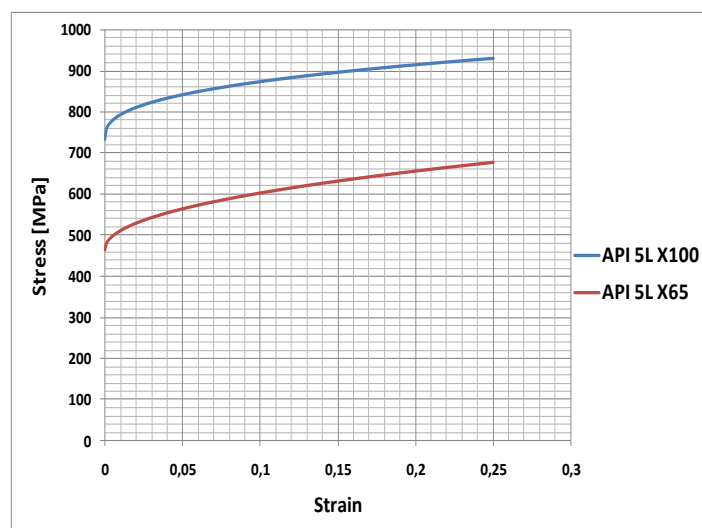


Fig.9 Stress strain curves of API 5L X65 and X100 pipe steels

Table 11 Yield stress and critical CTOA of
API 5L X65 and X100 pipe steels.

	CTOA _c [°]	σ _y [MPa]	n	D _{DWTT} (J)
API 5L X100	14	734	0.4793	160
API 5L X65	20	465	0.37	280

For API 5L X100 pipe steel, crack velocity curve have been computed with the critical CTOA taken from reference [15] were the thickness of the testing specimen is not specified. One note that the pressure -crack velocity curve is sensitive to the material fracture toughness as indicated in Fig 10.

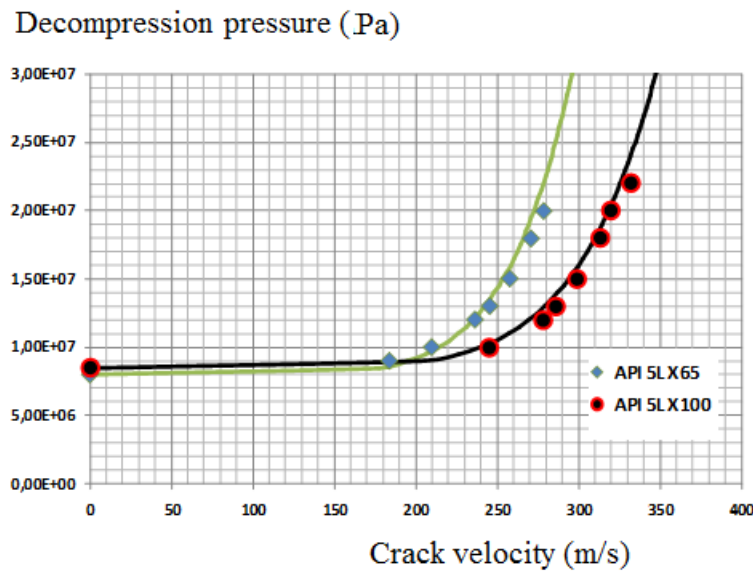


Fig.10 : Influence of material toughness on cack velocity curve, API5L X100 and X65 pipe steel.

The BTCM, HLP, HLP-Sumitomo Two Curves Method predictions of arrest pressure and crack extension are compared with these of modelled by Finite Element method using CTOA criterion. They are reported in Table 12 for arrest pressure and table13 for crack arrest length.

Table 12 Predictions of arrest pressure from BTCM, HLP ,HLP-Sumitomo and CTOA models for API5L X65 and X100 pipe steels.

Model	API 5L X65	API 5L X100
BTCM	p _{ar} = 5.55 MPa	p _{ar} =8.67 MPa
HLP	p _{ar} = 5.55 MPa	p _{ar} =8.67 MPa
HLP-Sumitomo	p _{ar} =5.55 MPa	p _{ar} =8.67 MPa
CTOA	p _{ar} = 8 MPa	p _{ar} =8.5 MPa

Table 13 Predictions of crack extension at arrest from BTCM, HLP ,HLP-Sumitomo and CTOA models at 40MPa pressure.

Model	API 5L X65 (m)	API 5L X100 (m)
BTCM	$a_{ar}= 26.30$	$a_{ar}= 26.27$
HLP	$a_{ar}= 73.55$	$a_{ar}= 66.45$
HLP-Sumitomo	$a_{ar}= 62.21$	$a_{ar}= 60.93$
CTOA	$a_{ar}= 55.47$	$a_{ar}= 62.55$

The CTOA model gives the highest arrest pressure for API 5L X65 pipe steel and p_{ar} is similar for all models and API 5L X100 pipe steel. Crack arrest is underestimated by BCM model and CTOA model gives the lowest arrest pressure for API 5L X65 pipe steel It is therefore less conservative or this steel. a_{ar} is similar for all models and API 5L X100 pipe steel. Comparison of CTOA, BTCM, HLP and HLP-Sumitomo Two Curves Methods for a pipe with outer diameter D 393 mm made in API 5L X 100 pipe steel indicates that HLP, HLP-Sumitomo and CTOA TCM pressure-crack velocity curve are very close (Fig. 11). For API 5L X 65 pipe steel, only curves obtain by HLP-Sumitomo is close to the curve obtain by CTOA model. HLP-Sumitomo two curves model has been establish for high strength pipe steel but is also a pertinent approach for medium strength steel as API 5L X 65.

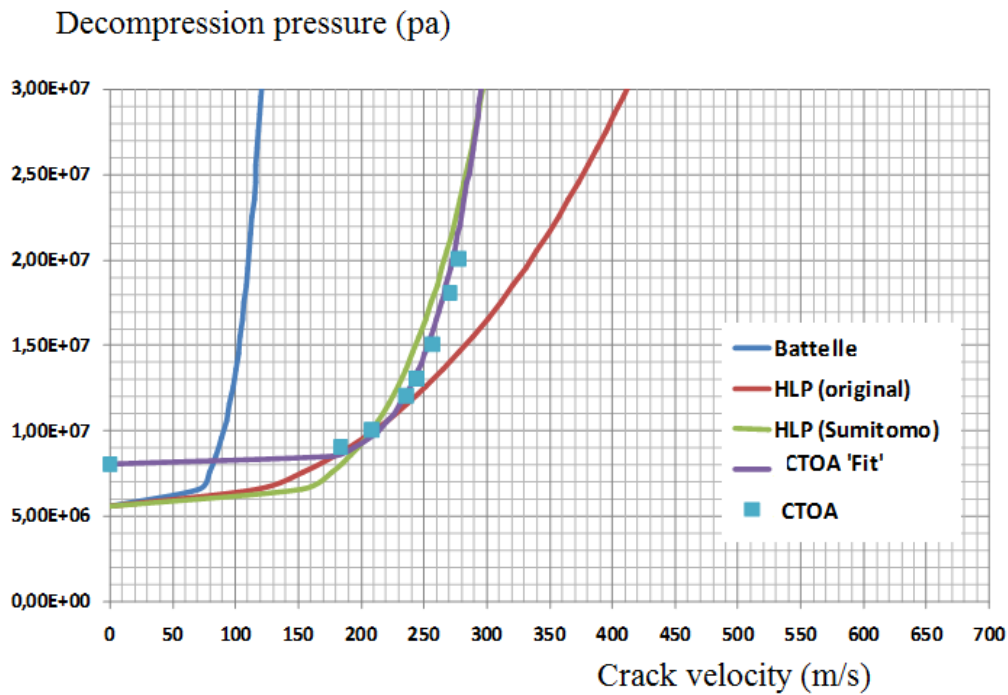


Fig.11 : Comparison of CTOA, BTCM, HLP and HLP-Sumitomo Two Curves Methods Pipe with outer diameter D 914.4 mm made in API 5L X65 pipe steel.

5.3 Influence on thickness on CTOA and arrest pressure

As a result of the parametric study, an interpolation formula for maximum CTOA has been developed for pipeline steels [16], this is given by the general form:

$$CTOA = C \left(\frac{\sigma_h}{E} \right)^m \left(\frac{\sigma_h}{\sigma_0} \right)^n \left(\frac{D}{t} \right)^q$$

m , n and q are dimensionless constants and C is in units of degrees, σ_h : hoop stress in units of MPa, σ_0 : flow stress in units of MPa, D : diameter in units of mm, t : thickness in units of mm. $h \sigma_0$ The following values can be used for methane: $C = 106$; $m = 0.753$; $n = 0.778$; $q = 0.65$.

CTOAc has been determined on 6 mm thick test specimen and the thickness of the pipe is 19 mm. Using equ.13, the corrected value of CTOAc is 9.5. Influence of CTOAc on arrest pressure has been determined and results have been presented in Fig 12. One notes that the influence of thickness on arrest pressure for API 5L X65 pipe steel (pipe diameter) is small and about 12% in the range 6-19 mm

Table 14 : Influence of thickness on predictions of arrest pressure. Pipe with outer diameter D 393 mm made in API 5L X 65 pipe steel

Thickness (mm)	CTOAc (°)	Pa (MPa)
6	20	23.1
19	9.5	20.5

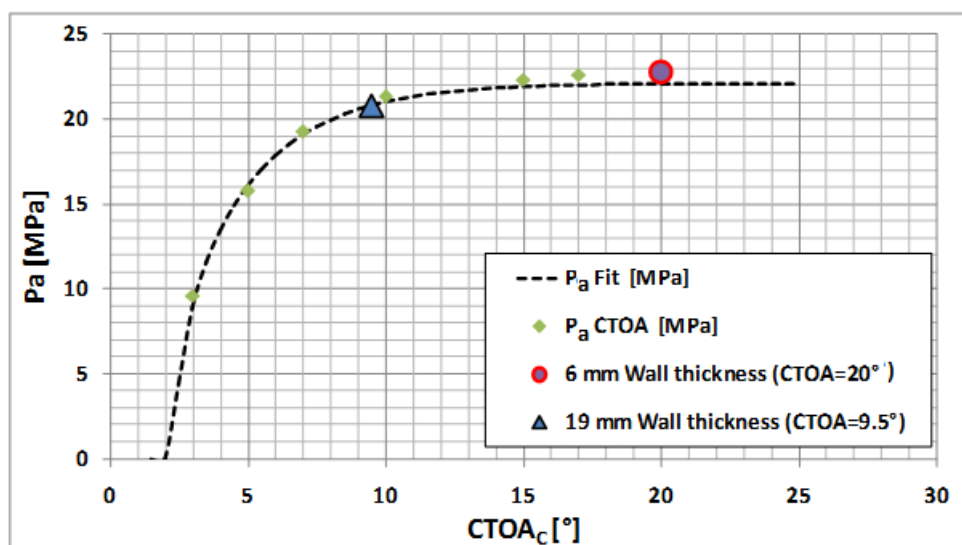


Fig 12 Influence of CTOAc on arrest pressure API 5L X 100 pipe steel.

It is well known now that fracture toughness (K_c or J_c) decreases when the thickness increases. The fracture toughness is maximal for plane stress conditions and trends asymptotically to a minimum called K_{Ic} or J_{Ic} if the plane strain conditions are satisfied. Therefore a description of fracture resistance cannot be done with a single parameter. Zhao and Guo [17] proposed to describe the effect of thickness B on fracture toughness $K_c = f(B)$ by introducing “a triaxial stress constraint” T_z .

This parameter is defined as:

$$T_z = \frac{\sigma_{zz}}{\sigma_{yy} + \sigma_{xx}} \quad (14)$$

For a straight crack through the thickness, which is a typical case of 3D cracks, y is the direction normal to the crack plane xoz. In an isotropic linear elastic cracked body, T_z ranges from 0 to N, $T_z = 0$ for the plane stress state, and $T_z = N$ for the plane strain state, where N is the strain hardening exponent of the Ramberg-Osgood strain-stress relationship. Values of T_z for the two pipe thickness are reported in Table 15 and compare with plane stress or plane strain stress states

Table 15 : triaxial stress constraint T_z values with pipe thickness.

Wall thickness [mm]	Internal diameter [mm]	T_z
Plane stress		0
6	355	0.204
10	355	0.2629
15	355	0.3109
19	355	0.335
Plane strain		1

5.3 Influence on pipe diameter on arrest pressure

According to BTCM, HLP and HLP-Sumitomo Two Curves Methods, the arrest pressure decreases with the square root of the diameter (see equ .8 and 11). Crack extension modelled by Finite Element method using CTOA criterion coupled with the the node release technique is used to predict arrest pressure in pipes of different diameters made in API 5L X65 steel with a 19 mm thickness. Results of arrest pressure predictions are reported in table 16 and compared with predictions of BTCM method. Data fitted by an exponential relationship between the arrest pressure and the square root of the pipe diameter exhibits a good correlation coefficient of $R_2 = 0.996$ which confirms the validity of this type of evolution. Table 16 confirms also that BTCM method underestimates the arrest pressure.

Table 16 : Evolution of arrest pressure with diameter APIX65 pipe steel

D [m]	P_a BTCM [MPa]	P_a CTOA [MPa]
0,30	21,5	29,00
0,39	16,7	22,30
0,61	10,7	14,50
0,91	7,0	9,70
1,22	5,2	7,20

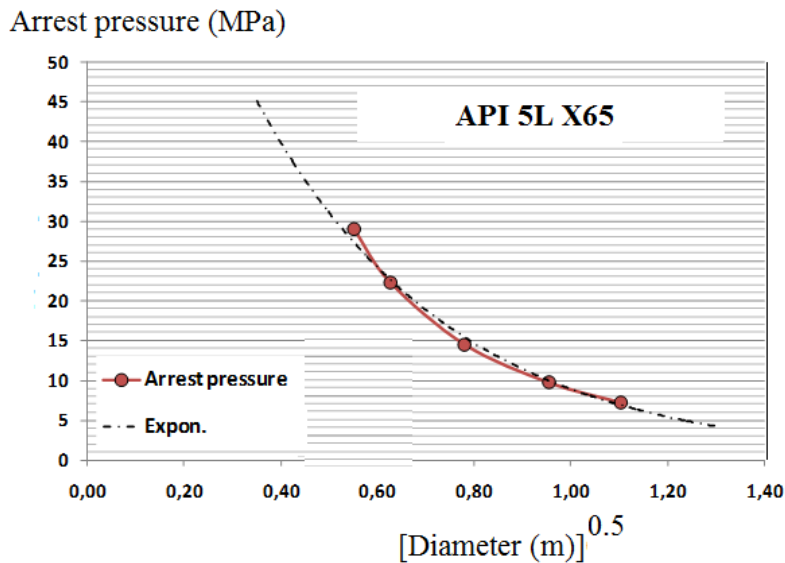


Fig.13 : Evolution of arrest pressure with square root of diameter.

CONCLUSION

In two curves methods as Batelle, HLP and HLP-Sumitomo, fracture resistance is described as specific fracture energy R_f . This paper mentions the difficulty to choose the ad hoc value for fracture toughness in either Charpy Vee energy or modified Charpy energy, DWTT energy from standard or embrittled specimens. It appears that the fracture resistance curve is not intrinsic to material but depends strongly of pipe geometry. To overcome these difficulties, we have proposed to use a fracture resistance curve based on CTOA which gives promising results but needs to be check with large scale burst tests. Attention needs to be paid on the effect of thickness and pipe diameter on crack arrest ability. This problem can be studied through a two parameters fracture approach CTOA-constraint.

REFERENCES

- [1] W. A Maxey. 5th Symp. on Line Pipe Research, PRCI Catalog No. L30174, Paper J, (1974).
- [2] E. Sugie, M. Matsuoka, H. Akiyama, T. Mimura, Y. Kawaguchi, "A study of shear crack-propagation in gas-pressurized pipelines", J. Press. Vess. – T. ASME 104 (4): 338–343, (1982).
- [3] D. Dawicke and M. Sutton, « CTOA and crack-tunneling measurements in thin sheet 2024-T3 aluminum alloy », Experimental Mechanics, vol. 34, no. 4, p. 357-368, déc. 1994.
- [4] J. Heerens and M. Schödel, « On the determination of crack tip opening angle, CTOA, using light microscopy and δ_5 measurement technique », Engineering fracture mechanics, vol. 70, no. 3-4, p. 417-426, 2003.
- [5] W. Lloyd and F. McClintock, « Microtopography for ductile fracture process characterization Part 2: application for CTOA analysis », Engineering Fracture Mechanics, vol. 70, no. 3-4, p. 403-415, févr. 2003.
- [6] Xu, N. Petri, et W. R. Tyson, « Evaluation of CTOA from load vs. load-line displacement for C(T) specimen », Engineering Fracture Mechanics, vol. 76, no. 13, p. 2126-2134, sept. 2009.

- [7] ASTM E2471-12e1, “Standard Test Method for Determination of Resistance to Stable Crack Extension under Low-Constraint Conditions”.
- [8] P.S. Lam, Y. Kim, Y.J. Chao, “The non-constant CTOD/CTOA ,instable crack extension under plane-strain conditions “, *Engineering Fracture Mechanics*, 73 (2006) 1070-1085.
- [9] O’Donoghue P.E, Kanninen M.F, Leung C.P, Demofonti G, Venzi S, The development and validation of a dynamic fracture propagation model for gas transmission pipelines, *Int. J. Pres. Ves. & Piping*, 70 : 11-25,(1997).
- [10] Ph. P. Darcis · C. N. Mccowan · J. D. Mccolskey · R. Fields crack tip opening angle measurement through a girth weld in an X100 steel pipeline section *Fatigue & Fracture of Engineering Materials & Structures* , 31(12) :1065 – 1078, (2008).
- [11] M.Ben amara , J.Capelle ,Z.Azari and G.Pluvinage” The application of CTOA criterion to simulate crack propagation and arrest in a modified CT test specimen”, Congress NT2F14” Belgrade Serbia, (2014).
- [12] Maxey, W., “Dynamic crack propagation in line pipe”, In: *Analytical and Experimental, Fracture Mechanics*, ed. Sih, G.C. and Mirabile, M., pages 109-123, (1981).
- [13] H.O. Nordhagen, S. Kragset, T. Berstad, A.Morin, C. Dørumb, S.T. Munkejord, “A new coupled fluid-structure modeling methodology for running ductile fracture”, *Computers and Structures* ,94-95 : 13-21, (2012).
- [14] Espen Jakobsen, “Deformation of pressurized pipelines”, Master Thesis, Norwegian University of Science and Technology, (2013).
- [15] Cheng Cen , “Characterization and calculation of fracture toughness for high grade pipes”, Thesis University of Alberta, (2013).
- [16] G. Demofonti, G. Mannucci, H.G. Hillenbrand, D. Harris, “Evaluation of the suitability Evaluation of X100 steel pipes for high pressure gas transportation pipelines by full scale tests”, *International Pipeline Conference*, Calgary, Canada, 2004.
- [17] Zhao J.& Guo W. “Three-parameter $K-T-T_z$ characterization of the crack-tip fields”in compact-tension-shear specimens”, *Engineering Fracture Mechanics*, Vol 92 : 72–88, (2012).